Response analysis of electron attachment rates to C3F8 and SF6 in buffer gases

Author(s):
Dahl, Dominik A.; Franck, Christian

Publication Date:
2013-11

Permanent Link:
https://doi.org/10.3929/ethz-b-000073709 →

Originally published in:
Journal of Physics D 46(44), http://doi.org/10.1088/0022-3727/46/44/445202 →

This is a post-refereeing copy of the manuscript submitted to IOP.

The original version can be found on the IOP web-page:
Digital Object Identifier: doi.org/10.1088/0022-3727/46/44/445202

Response analysis of electron attachment rates to C_3F_8 and SF_6 in buffer gases

Dominik A Dahl and Christian M Franck

High Voltage Laboratory, ETH Zurich,
CH-8092 Zurich, Switzerland

E-mail: `cfranck@ethz.ch`

Abstract. Electron swarm methods are applied for investigating the effects of small amounts ($\leq 1.5\%$) of a strongly electronegative sample gas in the buffer gases Ar, N_2 or CO_2. A pulsed Townsend method, a Monte Carlo swarm method, and a solution of the Boltzmann equation are used to determine the effective ionization rate constants of the gas mixtures. The sensitivity of the effective ionization rate constant to changes of the mixing ratio is evaluated. Our methods are benchmarked with the analysis of Ar-SF_6 and N_2-SF_6 mixtures, and subsequently used for the analysis of gas mixtures containing C_3F_8. The results based on the recommended C_3F_8 cross sections are shown to be inconsistent with the experimental data for N_2-C_3F_8 and CO_2-C_3F_8 mixtures.

PACS numbers: 52.80.Dy 51.50.+v 52.25.Fi

Submitted to: *J. Phys. D: Appl. Phys.*

1. Introduction

Gas mixtures containing strongly electronegative molecules are the medium for many industrial plasma processes, and for high voltage insulation and switching. Both these application domains require knowledge of the electron attachment parameters of electronegative molecules [1, 2]. One can investigate the attachment parameters of a sample molecule by means of swarm parameter measurements in buffer gases [3, 4, 5], when the relative concentration (mixing ratio) k of the sample molecule is small. In buffer gases with well known electron energy distribution (EEDF), like Ar, N_2 or CO_2, such experimental results are important for assessing the attachment cross sections of a sample molecule [3, 5, 6]. These experimental data can be applied more generally and readily, when the experimental technique achieves a separation between the swarm parameters of the buffer gas and the effects of the sample gas. For example, the swarm parameters of gas mixtures were evaluated for the rate constants of electron attachment to a sample molecule [3, 7]. However, these analyses were limited to such values of the reduced electric field strength E/N where ionization could be neglected. We aim for applying a similar technique also near the critical field strength $(E/N)_{\mathrm{crit}}$, where the

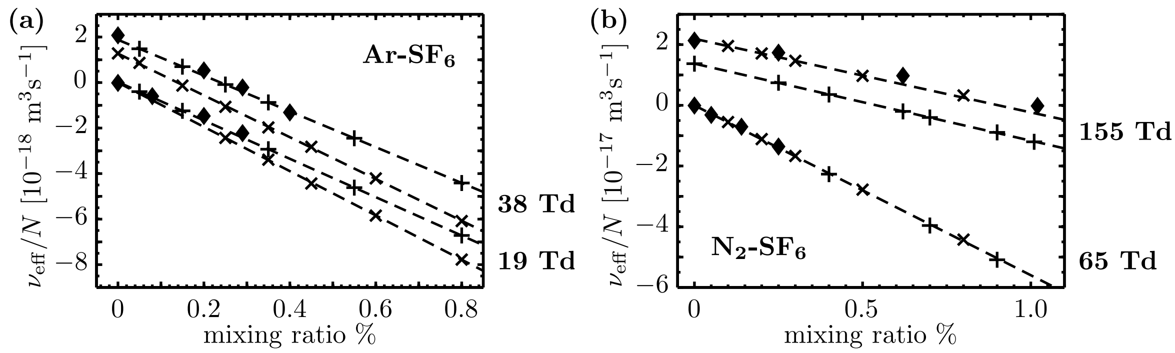

Figure 1. Measurements (♦) of the effective ionization rate constant, and the values (+) calculated by a Boltzmann solver [8] or (×) simulated by a Monte Carlo method [9] as a function of the mixing ratio of (a) SF_6 in Ar, and (b) SF_6 in N_2. The lines (− − −) represent the linear trends of the simulated or calculated values.

ionization rate equals the attachment rate, because this (E/N)-range is of particular interest for high voltage insulation technology.

For certain mixtures of an electronegative gas and a buffer gas, and for particular values of E/N, a linear relation is apparent between k and the effective ionization rate constant ν_{eff}/N. This is shown, for example, in figure 5 of [10] and figure 8 of [11]. Such a linear relation also appears in our measurements and in the results of two mutually independent numerical methods [8, 9], as one can note from the figures 1 and 6 of the present article.

Based on the assumption of a linear relation between ν_{eff}/N and k, we attempt to develop a linear response technique as a more convenient method for investigating the electron attachment parameters of sample molecules. This technique shall be tested with SF_6 which is a gas with well known parameter values [12]. SF_6 can therefore be considered as providing a benchmark [1, 13]. We compare our measurements to numerical results because experimental data are scarce in the parameter range of the present study [10, 11]. Subsequently, the linear response technique is applied for testing the attachment cross sections of octafluoropropane (C_3F_8).

1.1. Octafluoropropane

Previous work on C_3F_8 has been reviewed in [14, 15]. More recently, a new set of electron collision cross sections was derived from drift tube measurements [16], and the electron-impact dissociation cross sections were remeasured [17]. It is known that the electron attachment rate constant depends on the total gas density and the gas temperature. For 300 K and high total gas density, $\sim 10^{26}$ m^{-3}, the transient anion can be stabilized due to 3-body processes, and the non-dissociative attachment rate is comparable to the dissociative attachment rate. For higher temperatures > 500 K, only dissociative attachment was observed [18]. In consequence, the dissociative attachment cross section for 300 K was derived by extrapolating results obtained at elevated temperature. The present study is made at intermediate gas density, $\sim 10^{24}$ m^{-3}, at about 300 K, where our methods are not sensitive enough to detect a minor influence of density dependent processes. We argue that an independent test of the attachment cross sections is possible with the data of the present study.

2. Methods

2.1. Linear response technique

The effective ionization rate constant of a gas mixture $(\nu_{\mathrm{eff}}/N)_{\mathrm{k}}$ with mixing ratio k is defined by the EEDF $F_{\mathrm{k}}(\varepsilon)$ and by the ionization and attachment cross sections of the sample gas, $\sigma_{\mathrm{i}}(\varepsilon)$ and $\sigma_{\mathrm{a}}(\varepsilon)$ respectively, and the ionization minus the attachment cross sections of the buffer gas $\sigma_{\mathrm{B}}(\varepsilon)$, see also (10) in [8].

$$(\nu_{\mathrm{eff}}/N)_{\mathrm{k}} = \sqrt{\frac{2}{m_{\mathrm{e}}}} \int_0^\infty \varepsilon \left\{(1-k)\,\sigma_{\mathrm{B}} + k\,(\sigma_{\mathrm{i}} - \sigma_{\mathrm{a}})\right\} F_{\mathrm{k}} \mathrm{d}\varepsilon \ , \tag{1}$$

where m_{e} is the electron mass and

$$\int_0^\infty \sqrt{\varepsilon} F_{\mathrm{k}} \mathrm{d}\varepsilon = 1 \ .$$

We assume that $F_{\mathrm{k}}(\varepsilon)$ is very similar to the EEDF of the pure buffer gas $F_{\mathrm{B}}(\varepsilon)$:

$$F_{\mathrm{k}} \to F_{\mathrm{B}} \text{ for small } k \ . \tag{2}$$

Then (1) resolves to

$$(\nu_{\mathrm{eff}}/N)_{\mathrm{k}} \approx (\nu_{\mathrm{eff}}/N)_{\mathrm{B}} - k\sqrt{\frac{2}{m_{\mathrm{e}}}} \int_0^\infty \varepsilon \left\{\sigma_{\mathrm{B}} - \sigma_{\mathrm{i}} + \sigma_{\mathrm{a}}\right\} F_{\mathrm{B}} \mathrm{d}\varepsilon \tag{3}$$

$$(\nu_{\mathrm{eff}}/N)_{\mathrm{k}} \approx (\nu_{\mathrm{eff}}/N)_{\mathrm{B}} - k\, r_{\mathrm{BA}} \ , \tag{4}$$

with the effective ionization rate constant of the pure buffer gas $(\nu_{\mathrm{eff}}/N)_{\mathrm{B}}$, and the linear response parameter r_{BA}, which constitutes a characteristic property of a particular combination of a buffer gas B and a sample gas A.

Equation (4) evaluates the sensitivity of ν_{eff}/N on changes of k. It shall be used for obtaining r_{BA} as a function of E/N from calculated, simulated or measured ν_{eff}/N. One expects $r_{\mathrm{BA}} > 0$ for the sample gases and the E/N-range of the present study because the term σ_{a} predominates in the convolution integral (3).

2.1.1. Conditions for valid application. Assumption (2) holds only if the sample gas does not perturb the momentum and energy balance of the electron swarm [6, 19]. Only then it is valid to apply (3) for an interpretation of the linear response parameters. Otherwise, a perturbation of F_{B} must be taken into account when making a connection between $r_{\mathrm{BA}}(E/N)$ and $\sigma_{\mathrm{a}}(\varepsilon)$.

The influence of electron attachment on F_{B} can be neglected only if the attachment rate ν_{a} is much smaller than the total energy transfer rate [19]

$$\nu_{\mathrm{a}} \ll \frac{2m_{\mathrm{e}}}{M}\,\nu_{\mathrm{m}} + \sum_j \delta_j \nu_j \ , \tag{5}$$

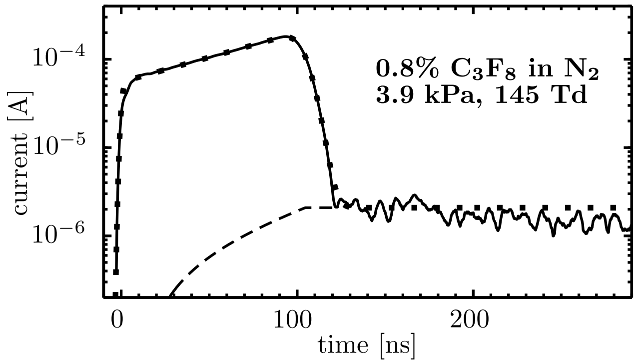

Figure 2. Logarithmic plot of measured swarm drift current (——) and a fit (······) of the swarm current model, which includes the ion current (– – –). The electrode spacing was $d = 15$ mm.

where M is the effective mass of the gas constituents, $\nu_{\rm m}$ is the momentum transfer collision rate, and ν_j are the rates of inelastic processes with fractional energy loss δ_j.

In particular gas mixtures, condition (5) may be violated, and electron attachment to the sample gas can strongly affect $F_{\rm B}$ even for small k. For example, such perturbations of $F_{\rm B}$ were previously found at $(E/N) \leq 20$ Td with 0.5% F_2 in Ar [20], or with 0.1% NF_3 in Ar [21]. For every particular combination of gases B-A, it is therefore necessary to test the range of E/N and k where a linear relation (4) can appear (see also sections 4.1.1 and 4.2.1).

2.2. Pulsed Townsend method

A pulsed Townsend (PT) electrical method is used. The experimental setup, its operation and the signal aquisition have not been modified since the original report [22]. The same methods are used here for recording the swarm drift currents and for evaluating the current waveforms. Four waveform parameters are obtained by fitting expressions derived from the usual swarm model [22] to the observed swarm drift currents:

- initial electron number
- swarm transit time T
- effective ionization rate $\nu_{\rm eff}$
- bulk diffusion time constant $\tau_{\rm D}$

These waveform parameters are treated by normalization techniques [22] in order to obtain $\nu_{\rm eff}/N$ and the bulk drift velocity w.

In the parameter range of the present study, the waveforms and the modelled swarm currents almost coincide. Figure 2 shows an excellent agreement between the measured and calculated currents.

2.3. Numerical methods and cross sections

For *simulating* electron transport parameters, we use a Monte Carlo (MC) method (Magboltz [9] version 9.0.1). The simulation settings were: 4×10^8 real collisions, total gas pressure 75 torr and temperature 297 K. Magboltz uses Itoh's cross section set for SF_6 [23], and proprietary sets for Ar, N_2, CO_2 and C_3F_8. We note that the proprietary dissociative attachment cross section of C_3F_8 closely corresponds to 0.85$\times$ the recommended cross section [14].

For *calculating* electron transport data, we use a solver (Bolsig+ [8] version 11.2011) for the 2-term expanded Boltzmann equation (BE) with a cross section database (SIGLO [24] version 11.2011). It includes Phelps' cross section sets for Ar and N_2 tested in [8], Morgan's set for CO_2, and Phelps' set for SF_6 [25]. The solver settings were: Precision 10^{-13}, Convergence 10^{-5}, Iterations 100, gas temperature 297 K, temporal growth model, equal energy sharing after ionization.

There are well known limitations of using 2-term BE methods for testing cross sections [5]. However, in the (E/N)-range under study, we argue that the 2-term BE method yields rate constants with satisfactory precision, provided that an accurate cross section set is available. It must be emphasized that the BE and MC methods are entirely different, and that their results are mutually independent because they are based on different cross section sets. Our choice of numerical methods and cross sections was made in order to provide disparate reference data for SF_6-mixtures.

3. Results

The present work concerns binary mixtures of one sample gas, SF_6 or C_3F_8, and one buffer gas, Ar, N_2 or CO_2. The purity of the gases and the mixing ratios under investigation are summarized in table 1. Table 2 specifies the ranges of total gas pressure for the measurements. We use the swarm parameters of N_2 and CO_2 from our previous study [22]. The data for Ar are given in table A1.

3.1. Mixture preparation

Gas mixtures were prepared directly in the experimental vacuum vessel which has a base pressure $< 10^{-5}$ Pa. After the vessel had been vented with the buffer gas B, the sample gas A was filled with the desired partial pressure. Then B was added to reach the desired total pressure. Gas pressure and temperature were continuously measured, and the total gas density N was determined at any time with uncertainty $\pm 1\%$ in the relevant pressure range 50 Pa to 11 kPa. Gas mixtures with $k < 0.5\%$ have been prepared starting from a mixture with $k = 0.5\%$ by pumping out part of the mixture and then refilling B to the desired total pressure.

Table 1. Mixing ratios of the sample gases, and the measured critical field strength of the gas mixtures. The gas purity is stated in brackets ($3.0 \equiv 99.9\%$).

	SF_6 (3.0)		C_3F_8 (4.0)	
buffer gas	mixing ratio %	$(E/N)_{crit}$ (Td)	mixing ratio %	$(E/N)_{crit}$ (Td)
Ar	0.08	30.5	0.17	25.3
(6.0)	0.20*	37.5	0.25	32.7
	0.29	41.0	0.51*	34.2
	0.40	43.5	1.01	40.2
N_2	0.05		0.09	79.0
(5.0)	0.14		0.37	93.8
	0.25*	129	0.81*	104
	0.62	144	1.51	113
	1.02	153		
CO_2			0.18	83.9
(5.0)			0.27	85.1
			0.81*	92.5
			1.21	95.8

* Tabulated swarm parameters given in the appendix.

3.2. Measurement parameters and procedures

The swarm parameter measurements were made at room temperature 293 to 300 K. After one measurement sequence was completed, the total pressure was reduced by pumping, and a subsequent measurement sequence was carried out. In this way the same gas mixture was investigated for 4 to 6 different N-values in the pressure range specified in table 2. The PT waveforms have been recorded for electrode spacings $d = (17, 15, 13, 11)$ mm in the E/N-range of interest. The cumulative uncertainty of the (E/N)-values was $\pm 1.5\%$.

The PT waveforms have been evaluated for the swarm parameters ν_{eff}/N and w. From the (ν_{eff}/N)-data the critical field strength $(E/N)_{\text{crit}}$ was determined by interpolation. The (ν_{eff}/N)-data of a pair of gases B-A with different k were plotted for selected values of E/N, as it is shown for example in figures 1 and 6. These plots served for checking the validity of a linear relation between ν_{eff}/N and k; refer to the discussion in sections 4.1.1 and 4.2.1. Finally, we applied (4) in order to obtain r_{BA}.

3.3. Data presentation

In table 2 the measurement parameters are specified for a gas mixture B-A, and the corresponding results are attributed.

3.3.1. ν_{eff}/N. The results of the effective ionization rate constant are classified by two columns of table 2. These columns denote

Table 2. Overview of the parameter range of measurements, and a catalogue of figure numbers where the results are presented. Refer to section 3.3 for column descriptions.

		ν_{eff}/N		r_{BA}		
buffer and sample gas	pressure (kPa)	overview (figure)	linearity (figure)	(E/N)-range (Td)	$\langle\varepsilon\rangle$-range (eV)	plot (figure)
Ar/SF_6	2 – 8	3	1(a)	19 – 43	5.51 – 6.00	5
N_2/SF_6	2 – 8	4	1(b)	40 – 165	1.11 – 4.27	5
Ar/C_3F_8	2 – 8		6(a)	22 – 46	5.61 – 6.06	7
N_2/C_3F_8	2 – 10.5		6(b)	20 – 150	1.03 – 3.85	7
CO_2/C_3F_8	2 – 9		6(c)	28 – 116	1.07 – 4.45	7

(i) a figure number where our measurements of ν_{eff}/N are plotted together with reference data.

(ii) a figure number where ν_{eff}/N was plotted as a function of k for selected values of E/N.

3.3.2. r_{BA}*.* The results of the linear response parameters are classified by three columns of table 2. These columns denote

(i) a range of E/N where r_{BA} was derived,

(ii) and the corresponding range of mean electron energies $\langle\varepsilon\rangle$ obtained with the MC simulation for the buffer gas.

(iii) a figure number where r_{BA} was plotted as a function of E/N.

The r_{BA}-results have been normalized to $k = 1\%$. The 95% confidence interval of r_{BA} is given as the error of the experimental data. In addition, the experimental data of $r_{\text{N2-C3F8}}$ and $r_{\text{CO2-C3F8}}$ are listed in table 3.

3.3.3. Supplemental results

- The experimental values of $(E/N)_{\text{crit}}$ are listed in table 1.
- For N_2-C_3F_8, selected experimental results of the reduced electron mobility $\mu N = wN/E$ are presented in figure 8.
- For selected mixtures, as indicated in table 1, the tabulated swarm parameters are given in the appendix.

4. Discussion

4.1. Benchmark with SF_6

4.1.1. Applicability of the method. In Ar-SF_6 mixtures, assumption (2) may be violated because $\sigma_{\text{a}}(\varepsilon \to 0\,\text{eV})$ is very large, and because the grand total cross section $\sigma_{\text{tot}}(\varepsilon \approx$

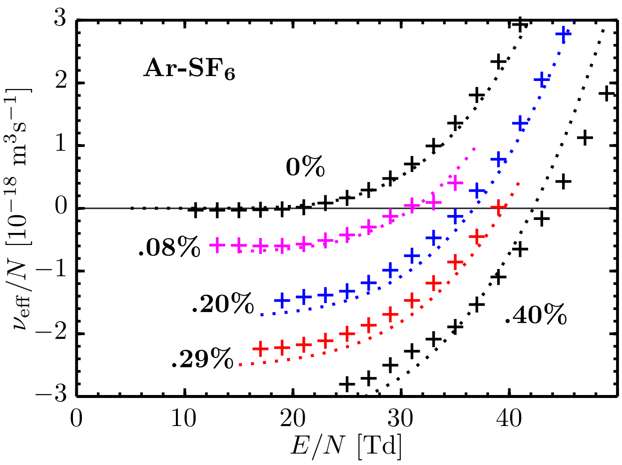

Figure 3. Measured (+) and BE-calculated (······) effective ionization rate constants $\nu_{\rm eff}/N$ in Ar-SF_6 for various mixing ratios.

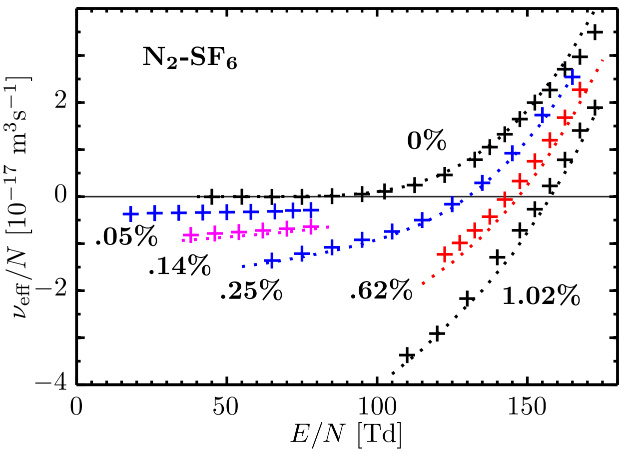

Figure 4. Measured (+) and MC-simulated (······) effective ionization rate constants $\nu_{\rm eff}/N$ in N_2-SF_6 for various mixing ratios.

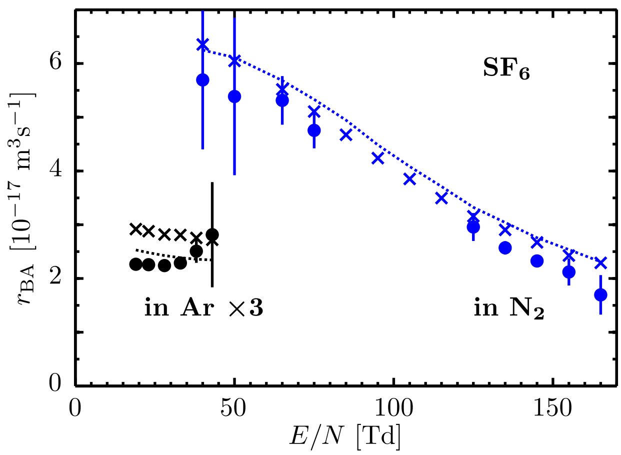

Figure 5. Measured (• with error |), MC-simulated (×) and BE-calculated (······) linear response $r_{\rm BA}$ of $\nu_{\rm eff}/N$ on adding 1% SF_6 into Ar or N_2. The data for Ar-SF_6 were multiplied by 3.

0.2 eV) is relatively small due to the Ar Ramsauer minimum. In N_2-SF_6 mixtures, assumption (2) may be violated for values of ε below the threshold of vibrational inelastic collisions with N_2. We argue that a perturbation of F_B only weakly affects ν_a in the parameter range of the present study, because the mean electron energy $\langle\varepsilon\rangle$ is sufficiently high, and condition (5) is met. The linear response method (4) may be applied in the (E/N)-range of the present measurements. A linear relation between $\nu_{\rm eff}/N$ and k is clearly observable in figure 1.

4.1.2. Assessment of results. At low E/N, e.g. 65 Td in N_2-SF_6 or 19 Td in Ar-SF_6, both numerical methods give results consistent with measured values, as it is apparent from figure 1. However, at higher E/N the $(\nu_{\rm eff}/N)$-results from BE and MC are significantly different from each other, probably because they employ somewhat different sets of cross sections. In the case of Ar-SF_6, our measurements agree fairly well with the BE-results, see also figure 3. In the case of N_2-SF_6, the measurements closely correspond to the MC-results, see also figure 4.

As one can see from figure 5, the BE- and MC-results nearly coincide on the values of $r_{\rm N2-SF6}$. The experimental data seem to be ∼5% smaller, but they qualitatively reproduce the BE- and MC-values. In the case of Ar-SF_6, the experimental results seem to be slightly smaller than the results of both numerical methods. We note that the cross section for the formation of SF_5^- was found to be much smaller than the ones used in the present calculations and simulations [13]. It might be necessary to adopt the cross sections from [13] in order to resolve the present small discrepancy between measurements and numerical results.

The response analysis of experimental $(\nu_{\rm eff}/N)$-data (figure 5) yielded relatively small errors when the analysis was based on at least four data points. Large uncertainties of $r_{\rm BA}$ appeared where the response analysis was based on three data points only, i.e. for 40 and 50 Td in N_2-SF_6, or for 43 Td in Ar-SF_6. These $r_{\rm BA}$-values with large uncertainties also seem to be qualitatively inconsistent with the reference values. It looks like the precision of experimental $r_{\rm BA}$-data is adequately represented by stating the 95%-confidence interval of the linear response parameter.

4.2. Test of the C_3F_8 attachment cross section

4.2.1. Applicability of the method. Figure 2 of [3] and figure 1 of [18] indicate a non-linear relation between k and the electron attachment rate constant ν_a/N_A, with N_A corresponding to the partial number density of C_3F_8. It should be noted that these values ν_a/N_A had been derived from measurements of the attachment coefficient η, using

$$\nu_a/N_A = \frac{\eta w_B}{N_A}\ , \qquad (6)$$

where w_B is the electron drift velocity of the buffer gas.

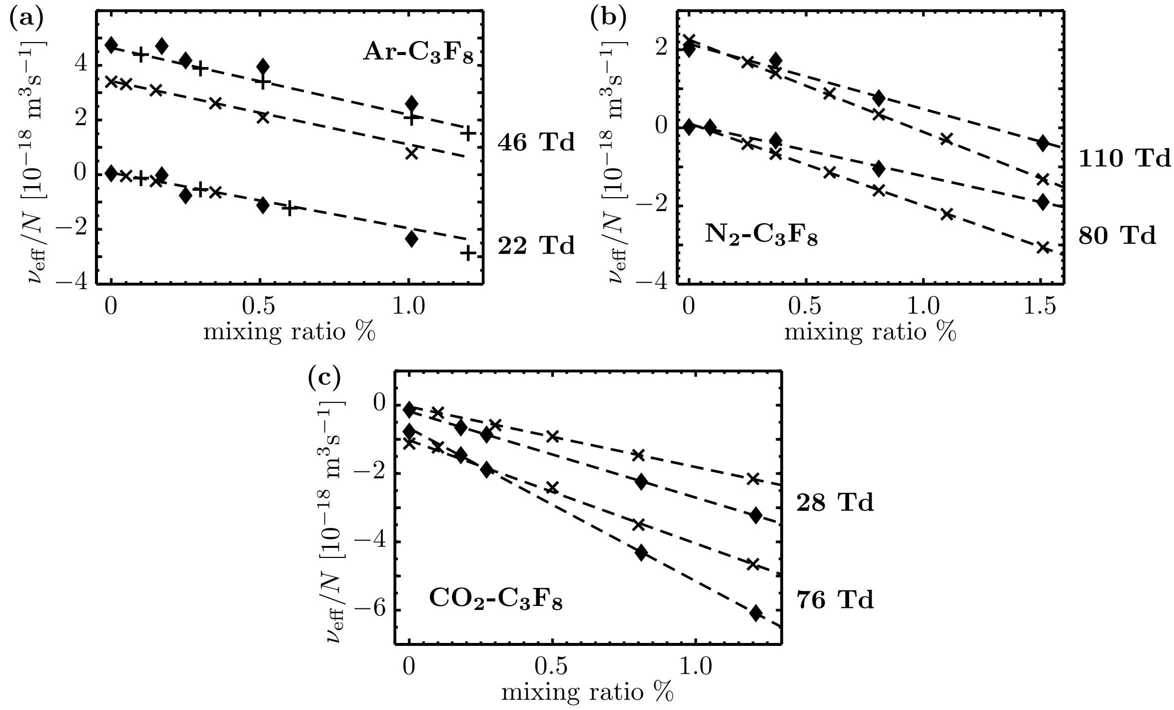

Figure 6. Measured (♦), BE-calculated (+) and MC-simulated (×) effective ionization rate constants in mixtures of (a) Ar-C_3F_8, (b) N_2-C_3F_8, and (c) CO_2-C_3F_8. The lines (– – –) represent a linear trend.

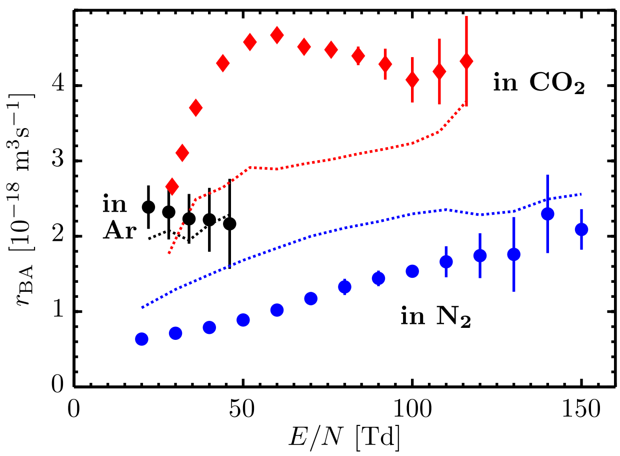

Figure 7. Measured (symbols with error |) and MC-simulated (······) linear response r_{BA} of ν_{eff}/N on adding 1% $\mathbf{C_3F_8}$ into Ar (•), N_2 (•) or CO_2 (♦).

It is apparent from figure 2 of [16] and from figure 8 of the present article that w significantly increases for $(E/N) < 40$ Td, when C_3F_8 is added into N_2 or Ar. We argue that the relation between η and k is non-linear because of the change of w with k.

In contrast, we measured ν_{eff}/N and found a linear relation between ν_{eff}/N and k for $k \leq 1.5\%$ in N_2, as one can note from figure 6(b). An application of the linear response method (4) seems to be permitted for the analysis of N_2-C_3F_8. In Ar buffer gas, see figure 6(a), the (ν_{eff}/N)-values for $k \approx 1\%$ seem to deviate from a linear trend.

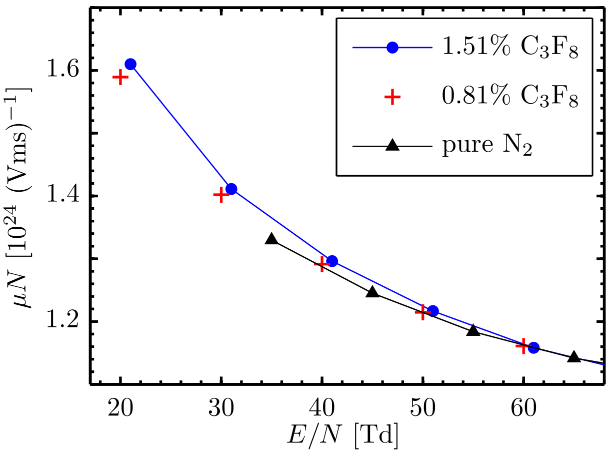

Figure 8. Pulsed Townsend results of the reduced electron mobility in N_2-C_3F_8 mixtures. The lines are merely for guiding the eye.

In consequence, the linear response analysis of Ar-C_3F_8 was restricted to $k \leq 0.51\%$.

In the case of CO_2-C_3F_8, assumption (2) seems to hold because both species have vibrational excitation cross sections with relatively low threshold energy. Then it is valid to apply (4).

4.2.2. Assessment of results. As shown in figure 7, our results for $r_{\mathrm{Ar-C3F8}}$ and the values from the MC simulation agree within the experimental uncertainty. The agreement indicates a suitable scaling of the total area of σ_a. The linear responses derived from the MC simulation for the N_2 or CO_2 buffer gases, however, are not consistent with the present experimental data. The experimental $r_{\mathrm{N2-C3F8}}$ are much *smaller* than the MC values. On the other hand, the experimental $r_{\mathrm{CO2-C3F8}}$ are much *larger* than the MC values.

In figure 7 the experimental data show a strong increase of $r_{\mathrm{CO2-C3F8}}$ between 30 and 50 Td. A maximum of $r_{\mathrm{CO2-C3F8}}$ appears near 60 Td. It is not present in the MC results. A monotonic increase of $r_{\mathrm{N2-C3F8}}$ with increasing E/N consistently appears in the experimental and simulated results. The uncertainty of the experimental response data is particularly large in such (E/N)-ranges where strong ionization occurs. In these (E/N)-ranges the experimental errors of k or E/N can strongly influence the measurement of ν_{eff}. In consequence, a relatively large scatter can appear in the corresponding (ν_{eff}/N)-values. The scatter causes a large 95%-confidence interval of the linear response parameter. For $(E/N) < 100$ Td, the precision of the experimental response data should be sufficient for testing revised attachment cross sections of C_3F_8.

5. Summary and conclusions

Electron swarm methods have been successfully applied for investigating the effects of small amounts of a strongly electronegative sample gas in a buffer gas. We evaluated the sensitivity of the effective ionization rate constant to changes of the mixing ratio.

Table 3. Linear response r_{BA} of ν_{eff}/N on adding 1% C_3F_8 into N_2 or CO_2.

E/N (Td)	$r_{\mathrm{CO2-C3F8}}$ ($10^{-18}\mathrm{m^3s^{-1}}$)	E/N (Td)	$r_{\mathrm{N2-C3F8}}$ ($10^{-18}\mathrm{m^3s^{-1}}$)
28	$2.52 \pm .04$	20	$0.63 \pm .15$
32	$3.11 \pm .04$	30	$0.72 \pm .07$
36	$3.71 \pm .07$	40	$0.80 \pm .07$
44	$4.30 \pm .07$	50	$0.90 \pm .08$
52	$4.58 \pm .03$	60	$1.03 \pm .08$
60	$4.67 \pm .02$	70	$1.17 \pm .11$
68	$4.51 \pm .02$	80	$1.33 \pm .14$
76	$4.48 \pm .04$	90	$1.45 \pm .18$
84	$4.39 \pm .12$	100	$1.57 \pm .23$
92	$4.28 \pm .20$	110	$1.67 \pm .43$
100	$4.08 \pm .30$	120	$1.74 \pm .62$
108	$4.19 \pm .43$	130	$1.75 \pm .99$
116	$4.32 \pm .60$	140	$2.25 \pm .84$
		150	$2.09 \pm .51$

The analysis yielded the linear response parameters as a function of the reduced electric field strength.

Our evaluation technique was benchmarked with an analysis of the effective ionization rate constants of SF_6-mixtures. The benchmark involved the results of our own pulsed Townsend measurements, the results of a well-approved Monte Carlo swarm method, and the results of a standard solver for the two-term expanded Boltzmann equation. We found satisfactory agreement between the linear response parameters derived from the results of the three different methods.

The linear response is a useful, characteristic parameter of gas mixtures. For example, the present technique can be applied for assessing electronegative additives for gas mixtures used in high voltage insulation applications. We gave directions for an interpretation of the linear response parameters with respect to the influence of the sample gas on the electron energy distribution in the buffer gas. A connection was made between the linear response parameters and the attachment cross sections of a sample molecule.

The linear response technique was applied for testing the attachment cross section of C_3F_8. For Ar, N_2 and CO_2 buffer gases, the linear response was simulated using a Monte Carlo swarm method with the recommended attachment cross sections. Experimental response data have been determined from our own pulsed Townsend measurements. As far as we know, the present work is the first report on swarm parameter measurements in CO_2-C_3F_8 mixtures. For the admixtures of C_3F_8 to Ar or N_2, our measurements of the effective ionization rate constant complement the data hitherto in the literature by expanding the range of mean electron energies covered.

The incompatibility of Monte Carlo simulations of electron attachment to C_3F_8 in N_2 or CO_2 with the experimental data indicates the necessity to re-assess the attachment cross sections of C_3F_8.

References

[1] Christophorou L G and Olthoff J K 2002 Electron interactions with plasma processing gases: present status and future needs *Applied Surface Science* **192** 309

[2] Christophorou L G and Pinnaduwage L A 1990 Basic physics of gaseous dielectrics *IEEE Transactions on Electrical Insulation* **25** 55

[3] Hunter S R and Christophorou L G 1984 Electron attachment to perfluoroalkanes n-C_NF_{2N+2} $N = 1 - 6$ using high pressure swarm techniques *J. Chem. Phys.* **80** 6150

[4] Rosa A, Barszczewska W, Foryś M and Szamrej I 2001 Electron capture by haloethanes in a carbon dioxide buffer gas *Int. J. of Mass Spectrometry* **205** 85

[5] Dupljanin S *et al* 2010 Transport coefficients and cross sections for electrons in N_2O and N_2O/N_2 mixtures *Plasma Sources Sci. Technol.* **19** 25005

[6] Bordage M C, Ségur P and Chouki A 1996 Determination of a set of electron impact cross sections in tetrafluoromethane consistent with experimental determination of swarm parameters *J. Appl. Phys.* **80** 1325

[7] Hunter S R, Carter J G and Christophorou L G 1989 Low energy electron attachment to SF_6 in N_2, Ar, and Xe buffer gases *J. Chem. Phys.* **90** 4879

[8] Hagelaar G J M and Pitchford L C 2005 Solving the Boltzmann equation to obtain electron transport coefficients and rate coefficients for fluid models *Plasma Sources Sci. Technol.* **14** 722 executable downloaded from http://www.bolsig.laplace.univ-tlse.fr/

[9] Biagi S F 1999 Monte Carlo simulation of electron drift and diffusion in counting gases under the influence of electric and magnetic fields *Nucl. Instr. and Meth. A* **421** 234 program source downloaded from http://magboltz.web.cern.ch/magboltz/

[10] Dincer M S, Ozerdem O C and Bektas S 2007 Effective ionization coefficients and transport parameters in ultradilute SF_6+N_2 mixtures *IEEE Trans. Plasma Science* **35** 1210

[11] Cekmen Z C and Dincer M S 2009 Effective ionization coefficients and transport parameters in binary and ultradilute SF_6-Ar mixtures using Boltzmann equation analysis *J. Phys. D: Appl. Phys.* **42** 145208

[12] Christophorou L G and Olthoff J K 2000 Electron interactions with SF_6 *J. Phys. Chem. Ref. Data* **29** 267

[13] Braun M, Marienfeld S, Ruf M-W and Hotop H 2009 High-resolution electron attachment to the molecules CCl_4 and SF_6 over extended energy ranges with the (EX)LPA method *J. Phys. B: At. Mol. Opt. Phys.* **42** 125202

[14] Christophorou L G and Olthoff J K 1998 Electron interactions with C_3F_8 *J. Phys. Chem. Ref. Data* **27** 889

[15] Christophorou L G and Olthoff J K 1999 Electron interactions with plasma processing gases: An update for CF_4, CHF_3, C_2F_6 and C_3F_8 *J. Phys. Chem. Ref. Data* **28** 967

[16] Jeon B-H 2006 Determination of electron collision cross-sections for the C_3F_8 molecule by using an electron swarm study *Journal of the Korean Physical Society* **49** 2321

[17] Baio J E *et al* 2007 Electron-impact dissociation cross sections for CHF_3 and C_3F_8 *J. Phys. D: Appl. Phys.* **40** 6969

[18] Spyrou S M and Christophorou L G 1985 Effect of temperature on the dissociative and nondissociative electron attachment to C_3F_8 *J. Chem. Phys.* **83** 2829

[19] Blevin H A, Fletcher J and Hunter S R 1985 Electron-velocity distribution functions in gases: The influence of anisotropic scattering and electron nonconservation by attachment and ionization *Phys. Rev. A* **31** 2215

[20] Dyatko N A *et al* 2000 On the possibility of negative electron mobility in a decaying plasma *J. Phys. D: Appl. Phys.* **33** 375

Table A1. Bulk velocity and effective ionization rate constant of Ar.

E/N (Td)	w (10^3 ms^{-1})	$\nu_{\rm eff}/N$ (10^{-18} m^{3}s^{-1})
11.0	10.6	$-0.03 \pm .01$
15.0	14.4	$-0.03 \pm .01$
19.0	18.0	$-0.02 \pm .01$
21.0	19.7	$0.02 \pm .01$
23.0	21.4	$0.08 \pm .01$
27.0	24.9	$0.29 \pm .01$
31.0	28.2	$0.71 \pm .01$
35.0	31.5	$1.36 \pm .02$
39.0	34.6	$2.34 \pm .03$
43.0	37.7	$3.59 \pm .05$
47.0	40.9	$5.14 \pm .06$
49.0	42.4	$5.76 \pm .07$

[21] Dyatko N A and Napartovich A P 1999 Electron swarm characteristics in Ar:NF_3 mixtures under steady-state Townsend conditions *J. Phys. D: Appl. Phys.* **32** 3169
[22] Dahl D A, Teich T H and Franck C M 2012 Obtaining precise swarm parameters from a pulsed Townsend setup *J. Phys. D: Appl. Phys.* **45** 485201
[23] Itoh H *et al* 1993 Electron transport coefficients in SF_6 *J. Phys. D: Appl. Phys.* **26** 1975
[24] Pancheshnyi *et al* 2012 The LXCat project: Electron scattering cross sections and swarm parameters for low temperature plasma modeling *Chem. Phys.* **398** 148
[25] Phelps A V and van Brunt R J 1988 Electron transport, ionization, attachment, and dissociation coefficients in SF_6 and its mixtures *J. Appl. Phys.* **64** 4269

Appendix A. Tabulated swarm data

PT measurements of the bulk velocity and the effective ionization rate constant are given for selected values of the reduced electric field strength E/N, which is in units of 1 Td $= 10^{-21}$ Vm^2.

The precision of the data is:

- $\pm 1.5\%$ experimental uncertainty of E/N.
- $\pm 0.5\%$ statistical uncertainty of w.
- The statistical uncertainty of $\nu_{\rm eff}/N$ is stated in the data tables.

The data for Ar (table A1) have been remeasured in order to cover a wider (E/N)-range than our previous measurements [22].

Table A2. 0.20% SF_6 in Ar.

E/N (Td)	w (10^3 ms^{-1})	$\nu_{\rm eff}/N$ (10^{-18} m^{3}s^{-1})
19.0	17.9	$-1.47 \pm .01$
21.0	19.7	$-1.41 \pm .01$
23.0	22.0	$-1.38 \pm .01$
27.0	25.3	$-1.19 \pm .01$
31.0	28.2	$-0.76 \pm .01$
35.0	31.5	$-0.13 \pm .02$
37.0	33.0	$0.28 \pm .02$
41.0	36.1	$1.36 \pm .03$
45.0	39.9	$2.78 \pm .05$
47.0	41.4	$3.51 \pm .06$
49.0	43.1	$4.55 \pm .07$

Table A3. 0.51% C_3F_8 in Ar.

E/N (Td)	w (10^3 ms^{-1})	$\nu_{\rm eff}/N$ (10^{-18} m^{3}s^{-1})
22.0	23.0	$-1.12 \pm .01$
26.0	25.5	$-0.90 \pm .01$
30.0	28.0	$-0.47 \pm .01$
34.0	30.9	$0.12 \pm .01$
38.0	33.8	$1.03 \pm .02$
42.0	37.3	$2.31 \pm .03$
46.0	40.8	$3.95 \pm .04$
50.0	43.8	$5.56 \pm .05$
54.0	47.0	$7.55 \pm .07$

Table A4. 0.25% SF_6 in N_2.

E/N (Td)	w (10^3 ms^{-1})	$\nu_{\rm eff}/N$ (10^{-18} m^{3}s^{-1})
65.0	73.9	$-13.6 \pm .1$
75.0	83.5	$-12.1 \pm .1$
85.0	93.7	$-10.8 \pm .1$
95.0	104	$-9.19 \pm .04$
105	114	$-7.42 \pm .03$
115	123	$-4.99 \pm .04$
125	134	$-1.61 \pm .07$
135	144	$2.92 \pm .10$
145	155	$9.22 \pm .15$
155	165	$17.3 \pm .2$
165	176	$25.4 \pm .3$

Table A5. 0.81% C_3F_8 in N_2.

E/N (Td)	w (10^3 ms^{-1})	ν_{eff}/N (10^{-18} m^{3}s^{-1})
20.0	31.8	$-0.61 \pm .01$
30.0	42.0	$-0.68 \pm .01$
40.0	51.6	$-0.75 \pm .01$
50.0	60.7	$-0.83 \pm .01$
60.0	69.6	$-0.92 \pm .01$
70.0	78.5	$-1.01 \pm .01$
80.0	87.6	$-1.05 \pm .01$
90.0	97.1	$-0.89 \pm .01$
100	107	$-0.36 \pm .01$
110	117	$0.76 \pm .02$
120	128	$2.72 \pm .05$
130	138	$5.75 \pm .08$
140	149	$10.4 \pm .2$
150	159	$16.7 \pm .2$

Table A6. 0.81% C_3F_8 in CO_2.

E/N (Td)	w (10^3 ms^{-1})	ν_{eff}/N (10^{-18} m^{3}s^{-1})
20.0	60.9	$-1.15 \pm .01$
28.0	85.1	$-2.24 \pm .03$
36.0	96.9	$-3.25 \pm .03$
44.0	104	$-3.99 \pm .02$
52.0	110	$-4.57 \pm .03$
60.0	116	$-4.99 \pm .03$
68.0	121	$-4.95 \pm .02$
76.0	127	$-4.32 \pm .02$
84.0	132	$-2.83 \pm .03$
92.0	137	$-0.21 \pm .02$
100	143	$3.56 \pm .07$
108	149	$8.75 \pm .11$
116	155	$15.8 \pm .2$